



Published in final edited form as:

*J Biomed Mater Res A*. 2017 May ; 105(5): 1252–1259. doi:10.1002/jbm.a.35984.

## Chitosan Nanofibers for Transbuccal Insulin Delivery

Michael G. Lancina III<sup>1</sup>, Roopa Kanakatti Shankar<sup>2</sup>, and Hu Yang<sup>3,4,5,\*</sup>

<sup>1</sup>Department of Biomedical Engineering, Virginia Commonwealth University, Richmond, Virginia 23284, United States

<sup>2</sup>Division of Endocrinology, Children's Hospital of Richmond at VCU, Center for Endocrinology, Diabetes and Metabolism, Virginia Commonwealth University, Richmond, Virginia 23229, United States

<sup>3</sup>Department of Chemical and Life Science Engineering, Virginia Commonwealth University, Richmond, Virginia 23219, United States

<sup>4</sup>Department of Pharmaceutics, Virginia Commonwealth University, Richmond, Virginia 23298

<sup>5</sup>Massey Cancer Center, Virginia Commonwealth University, Richmond, Virginia 23298

### Abstract

**Purpose**—In this work, we aimed at producing chitosan based nanofiber mats capable of delivering insulin via the buccal mucosa.

**Methods**—Chitosan was electrospun into nanofibers using poly (ethylene oxide) (PEO) as a carrier molecule in various feed ratios. The mechanical properties and degradation kinetics of the fibers were measured. Insulin release rates were determined in vitro using an ELISA assay. The bioactivity of released insulin was measured in terms of Akt activation in pre-adipocytes. Insulin permeation across the buccal mucosa was measured in an ex-vivo porcine transbuccal model.

**Results**—Fiber morphology, mechanical properties, and in vitro stability were dependent on PEO feed ratio. Lower PEO content blends produced smaller diameter fibers with significantly faster insulin release kinetics. Insulin showed no reduction in bioactivity due to electrospinning. Buccal permeation of insulin facilitated by high chitosan content blends was significantly higher than that of free insulin.

**Conclusions**—Taken together, our work demonstrates chitosan based nanofibers have the potential to serve as a transbuccal insulin delivery vehicle.

### Keywords

electrospun fiber; chitosan; insulin; transbuccal delivery

---

\*Correspondence should be addressed to Hu Yang, Department of Chemical and Life Science Engineering, Virginia Commonwealth University, 737 North 5<sup>th</sup> Street, Biotech 8, Richmond, Virginia 23219, United States. Tel.: 1-804-828-5459; Fax: 1-804-828-4454; hyang2@vcu.edu.

## Introduction

As of 2011, almost 6 million Americans were already using exogenous insulin to manage diabetes, and the majority of these patients administered insulin through invasive means, usually subcutaneous injection or infusion pump (1). These methods, however, may cause serious side effects including, but not limited to, allergic reactions and lipohypertrophy (2). Importantly, neither is an optimal solution for pediatric patients, a rapidly growing group (3, 4), for whom insulin is the mainstay of diabetes therapy. These problems and the poor patient compliance associated with them have driven considerable research into alternative delivery methods, including oral, nasal, and pulmonary therapies (5). There are obvious advantages of oral insulin delivery compared to injections, but enzymatic and chemical processes in the GI tract limit the bioavailability of orally delivered insulin to a degree where traditional drug delivery materials and methods are not viable (6). One possible solution to this problem is to bypass the GI tract and hepatic portal system by absorbing insulin through the oral mucus membranes (7–10). A material capable of enhancing rapid uptake of insulin across the buccal mucosa would be able to combine the rapid and predictable dosing of subcutaneous injection with the patient comfort and safety of a pill.

The buccal mucosa itself is comprised of a layer of epithelial cells around 40–50 cells thick that make up the inner lining of the cheeks (11). Besides its ready accessibility, several other aspects of this tissue make it an attractive drug delivery route. The buccal mucosa is estimated to be as much as 4000 times more permeable than skin epithelium (11). The area is highly vascularized, so absorbed materials reach the systemic circulation rapidly. Also, cell growth is very rapid, with complete turnover occurring every 5–8 days, limiting any acute cytotoxic effects caused by high drug concentrations at the delivery site (12). Despite these advantages, hydrophilic drugs and especially proteins do not usually diffuse across the mucosa fast enough for this to serve as a viable alternative to subcutaneous injection. Common strategies to increase transbuccal drug delivery include permeation enhancers that loosen the junctions between epithelial cells and mucoadhesive polymers capable of holding compounds at high local concentrations long enough to allow diffusion to take place, but very few materials meet the level of biocompatibility necessary to be used for long term insulin therapy.

Chitosan (CS), is one such material. Chitosan is the partially N-deacetylated derivative of chitin, the major structural component of crustacean and insect shells. While similar to other structural polysaccharides such as cellulose in both biocompatibility and natural abundance, chitin is uniquely cationic. The combination of these properties makes it an attractive research target in a number of diverse biomedical applications including transmembrane drug delivery. This work is hindered by chitin's insolubility in most solvents, but Processing into CS somewhat improves the solubility of the material. Once dissolved, nanofabrication methods such as electrospraying or electrospinning can produce materials capable of transmembrane drug delivery (13). CS based nanoparticles have been investigated for oral insulin delivery by several groups (14–20), but there are physical limitations to handling and packaging nanoparticles. Electrospun fibers on the other hand have many of the advantageous physical properties of polymeric films and textiles while maintaining the high

surface area to volume ratios of nanoparticles that make them such potent drug delivery vehicles.

In this work we have developed electrospun chitosan fibers blended with polyethylene oxide (PEO). The fiber diameter, mechanical properties, degradation rates, and insulin release kinetics of these fiber blends were first characterized. To ensure insulin entrapped in the fibers remains bioactive during the electrospinning process, Akt-1 phosphorylation in pre-adipocytes exposed to CS fiber scaffolds was quantified. An ex-vivo porcine model was used to measure the buccal permeability of insulin released from each fiber blend. The results presented herein support that this new formulation has the potential to serve as a cost effective platform for transbuccal insulin delivery.

## Materials and Methods

### Materials

Chitosan (CS, product#448869, batch#SLBH5874V), poly (ethylene oxide) (PEO, MW 900kDa, product#189456 batch#0741DD), and human insulin (INS, lyophilized powder, product#I2643, batch#SIBK6641V) were purchased from Sigma Aldrich (St. Louis, MO). 1,1,1,3,3,3-hexafluoro-2-propanol (HFP) was purchased from Oakwood Chemicals (Estill, SC). Insulin ELISA assay kit (product#IS130D) was purchased from Calbiotech (Spring Valley, CA).

### Electrospun fiber production

CS and PEO were dissolved in HFP at the concentrations indicated in Table 1. The solution was stirred for 72 hours at room temperature, allowing all solid components to completely solubilize. INS was then added at a final concentration of 0.4 mg/ml. At the given concentration, insulin dissolved rapidly to produce a translucent solution of uniform color and viscosity. The solution was electrospun into solid fiber mats under the following conditions: 15 kV DC offset, 17 cm air gap, 18 ga. blunted needle, and 3 ml/h flowrate. A typical spinning run used 5 ml of solution and a round collecting mandrel (6.5 mm diameter). Scaffolds were dried under vacuum 3 hours to remove residual solvent before any further testing.

### Mechanical tests

Uniaxial tensile testing of electrospun scaffolds was performed as previously described (21, 22). Briefly, dogbone shaped punches of all fiber blends were taken longitudinally oriented with the predominant fiber alignment. Scaffold thickness over the gauge length was measured with precision calipers and the samples were loaded into a MTS Bionix 200 testing frame. Samples were uniaxially extended at 10mm/min until failure.

### *In vitro* stability

Fiber stability under physiologic conditions was assessed quantitatively by mass loss and qualitatively by SEM imaging. Briefly, 10 mg fiber samples were incubated in 1 ml of PBS at 37°C. At predetermined time points, the samples (n = 3) were spun down and the degradation media removed. Scaffolds were then washed briefly in diH<sub>2</sub>O, lyophilized and

weighed. One sample from each time point was then mounted and gold coated for SEM imaging. SEM images were taken on a JEOL LV-5610 scanning electron microscope. The diameters of fabricated fibers were measured by using ImageJ software, to analyze at least 150 randomly chosen fibers in each SEM image as previously reported (23, 24).

### ***In vitro* insulin release**

Circular samples 8mm in diameter of each fiber blend were weighed and hydrated in 10 ml of phosphate buffered saline at 37°C. At specified time points the tubes were vortex stirred briefly and 100 µL samples taken of the release medium. A sandwich ELISA assay was then used to quantify insulin concentrations.

### **Insulin bioactivity**

To ensure insulin was not denatured during electrospinning Akt phosphorylation of cells exposed to fiber release media was measured by western blot. 3T3-L1 preadipocyte cells were seeded in 6-well tissue culture plates and allowed to reach confluence. Growth medium was removed and replaced with either fresh growth medium, insulin containing medium (200 µIU/ml), or fiber release medium (CS:PEO20 0.15mg/mL for 6 hours). After incubating for 10 minutes at room temperature, cells were lysed and western blot analysis was performed as previously described (22). Briefly, cell lysates were separated on an SDS-PAGE gel (10% w/v) and transferred onto a PVDF membrane using Bio-Rad Mini-Blot transfer apparatus. The membrane was blocked for 2 h in Tris-buffered saline (TBS) containing non-fat dried milk (5% w/v). Phosphorylated Akt-1 on the membrane was determined by incubating with a primary antibody overnight at 4 °C with shaking. The membrane was washed and then incubated in a 1:3000 dilution of a secondary antibody at room temperature for 1 hour in washing buffer (TBS containing 0.5% w/v Tween 20). The specific antigen-antibody interactions were detected using enhanced chemiluminescence. The membranes were then stripped and re-probed for total expression of Akt-1 to use as the loading control.

### **Transbuccal permeation**

Fresh porcine heads were purchased from Animal Biotech Industries (Danboro, PA). Immediately upon arrival buccal membranes were removed and cleaned of any loose connective or adipose tissue to a thickness of approximately 1mm. Buccal membranes were loaded into a Franz diffusion cell (PermeGear, Cranford, NJ) with the epithelial side facing the donor chamber. The acceptor chamber was filled with 5.2 ml of PBS and maintained at 37 °C. A 10mm fiber sample was placed on the buccal tissue in the donor chamber and 0.5 ml of simulated salival fluid (SSF) was added (25). At predetermined time points 100 µl samples were taken from the acceptor chamber and the fluid was replaced with fresh PBS. The insulin concentration in the acceptor chamber fluid was measured using ELISA assay as previously described. The permeability coefficient, *P*, of insulin was calculated using the following equation:

$$P = \frac{dQ/dt}{AC}$$

where  $dQ/dt$  is the steady-state slope of a cumulative flux curve,  $C$  is the loading concentration of insulin in the donor chamber, and  $A$  is the effective cross-sectional area ( $0.785 \text{ cm}^2$ ) available for diffusion (19).

### Statistical analysis

All the data are expressed as mean  $\pm$  standard error. Significant differences were determined using a one way analysis of variance followed by a one sided Students t-test in JMP software.

## Results

### Electrospun fiber production

Electrospinning of neat chitosan was not successful due to the lack of sufficient chain entanglements (26). The addition of PEO enabled production of smooth fibers. But mixed beading due to fiber rupture was observed at polymer concentrations less than 20% (wt/wt). A mixed population of sub-micron ( $\sim 200 \text{ nm}$ ) and larger ( $1\text{--}2 \mu\text{m}$ ) fibers were seen under SEM for high PEO content blends (Figure 1). Mandrel shape was important in producing fiber mats with consistent thickness and density and an even distribution of insulin throughout the fibers. Early experiments using a flat rectangular mandrel showed wide variability in both the thickness of fibers deposited and the weight ratio of insulin trapped within the fibers. Both of these problems were corrected by switching to a cylindrical collecting mandrel. Mechanical tests confirmed mechanical properties of the fibers changed predictably with the composite ratios of CS and PEO. High CS content fibers showed a significantly higher maximum stress but also a reduced strain at failure compared to the more ductile high PEO blends (Table 2).

### Physiological stability

Mass measurements and SEM micrographs were used to evaluate how fiber mats degraded when hydrated. These experiments showed CS:PEO fiber solubility in physiologic conditions can be predicted by blend ratio (Figure 2A). When hydrated fibers lose most of their bulk mass of PEO within 15 minutes, but show no significant mass loss over the next 6 hours. SEM images were consistent with these measurements, with significant changes in fiber diameter from 0 to 15 minutes, but no changes for the duration of the degradation period (Figure 2B&C).

### *In vitro* insulin release

Short and long term insulin release under physiologic conditions was measured for all fiber blends. Insulin release kinetics was highly dependent on the polysaccharide content of electrospun fiber mats (Figure 3). Higher chitosan content blends released insulin significantly faster than lower chitosan content blends. By six hours CS:PEO20 and CS:PEO33 blends showed no significant difference and by 24 hours all fibers showed the same level of insulin release. The release profile for all three fiber blends could be fit to a simple model of Fickian diffusion, and the fit was not improved by incorporating a term for scaffold degradation (Table 3).

### Insulin bioactivity

3T3L-1 preadipocytes treated with 6 hour release medium showed significantly greater ratio of activated Akt than both negative (culture medium) and positive (insulin containing) controls (Figure 4). This indicates there is no loss of insulin bioactivity due to dissolution in HFP, electrospinning, or dry storage at room temperature for several weeks.

### Buccal permeation

High chitosan content is needed to induce transbuccal insulin delivery. Lower chitosan content blends CS:PEO50 and CS:PEO33 did not outperform dissolved insulin in the 6 hour test, although all three groups saw negligible concentrations of transbuccal insulin (less than 1% of the total) (Figure 5). CS:PEO20 fibers on the other hand delivered on average around 1/3 of their total insulin into the acceptor chamber after 6 hours. Permeability coefficients for the lower chitosan content blends were 5 and 10 fold lower than naked insulin respectively while CS:PEO20 fibers had a permeability coefficient over 10 fold higher than the same control (Table 4).

## Discussion

### Electrospun fiber production

In this work we developed chitosan-based electrospun fiber scaffolds for oral insulin delivery. Nanostructured materials benefit from extremely high surface area to volume ratios that provide more space for both drug diffusion and interaction with the given biologic environment or surface. Transbuccal insulin delivery is an ideal application to take advantage of these properties. Chitosan-based nanoparticles have shown promise in a number of transbuccal drug delivery applications, but there are practical drawbacks to producing and utilizing nanoparticles in a clinical setting. Electrospun fiber mats overcome many of these physical limitations by combining the workability of polymer films with the high surface area of nanoparticles. The structure of chitosan however presents several problems for electrospinning. Solubility was the first hurdle, as the solvent system used needed to efficiently dissolve chitosan without denaturing insulin. A number of solvent systems have been investigated for electrospinning pure chitosan, most commonly dilute acetic acid solutions but insulin is known to rapidly lose bioactivity at low pH (27). Highly polar fluorinated solvents, such as HFP had previously been shown to readily dissolve chitin and chitosan, as well as insulin without permanent structural changes (22, 28). Neat chitosan solutions in HFP can be readily electrospayed into nanoparticles, but the rigid, charged polysaccharide molecules do not readily form the chain entanglements that are needed for stable fiber formation (29). High-molecular-weight PEO is readily electrospun, has excellent biocompatibility, and has been theorized to form hydrogen bonds with the amine groups on chitosan (26). These hydrogen bonds encourage the chain entanglement that improve the overall spinning efficiency of the polymer solution, but also significantly increases the fiber diameter of the final composite fiber material. Preliminary work then focused on finding the minimum amount of PEO needed to reliably form composite fiber scaffolds, and characterizing the material properties of different CS:PEO blend ratios. CS:PEO50 and CS:PEO33 blends efficiently produced mats of continuous fibers as previously reported (30). At blend ratios with lower PEO content than CS:PEO20 fibers ruptured before solidifying, a

phenomenon known as beading. Beading was intermittent in CS:PEO20 mats but could be minimized by adjusting spinning parameters.

Mechanical tests confirmed the composition of deposited fiber scaffolds matched that of the initial spinning solution, and neither component was disproportionately lost during fiber formation. As expected, increasing polysaccharide concentration in the spinning solution resulted in more brittle fiber scaffolds, with an increased peak stress and decreased strain at failure.

For this work, it was desirable for fibers to adhere, swell, and release loaded insulin but not to degrade significantly over the 3–6 hours they will be attached to the application site. While both components of the scaffolds have very good biocompatible properties it is always still preferable to limit the amount of polymer delivered into the circulation in case there are any unknown tissue specific effects or unanticipated drug interactions. Degradation experiments show when hydrated the different CS:PEO blends lose approximately 15, 20, and 50% of their bulk mass rapidly depending on the blend ratio, but there is no significant mass loss over the next 6 hours. This suggests the majority of PEO incorporated into the fiber mats dissolves rapidly leaving behind primarily chitosan fibers. While chitosan is stable enough in aqueous solvents that no significant amount dissolves during the test period, the dissolution of PEO does appear to have a major impact on the final morphology of the fiber mat. Prior to hydration, median fiber diameter was not dependent on blend ratio, but when hydrated higher PEO content blends saw a significantly larger increase in fiber diameter. This means while all three fiber blends may have a similar chemical composition a few minutes after application, they maintain unique physical properties.

After material characterization, the insulin release kinetics of the fibers needed to be measured. Although there are applications for long-acting insulin, for oral delivery it is not realistic to expect a material to stay in place for more than a few hours. This makes it critical for a transbuccal delivery vehicle to have quick, predictable insulin release. With the two phases of degradation occurring over the test period, there were two likely mechanisms of insulin release out of the fibers: rapid dissolution along with PEO and slow diffusion out of the stable CS microfibers. If rapid dissolution along with PEO dominated, CS:PEO50 would have the fastest insulin release kinetics due to the large amount of mass those fibers lose. On the contrary, if diffusion out of the fibers was the primary mechanism, CS:PEO20 would have the most rapid insulin release because those fibers have the greatest surface area for diffusion to take place. The results observed showed diffusion is the dominant mechanism at all time points, with the low PEO content blend showing the highest insulin release at 15 minutes despite undergoing the smallest amount of fiber morphological changes. This conclusion is further supported by fitting several common models of soluble drug release to the data (31). The simplest equation to fit the data reasonably well for all three materials was the Ritger-Peppas model which has the form:

$$M_t/M_\infty = kt^n$$

where the fractional drug release ( $M_t/M_\infty$ ), is determined by a kinetic constant  $k$ , and a diffusional exponent  $n$  (32). Use of a more complex model such as the Peppas-Sahlin equation which has the form:

$$M_t/M_\infty = k_1 t^m + k_2 t^{2m}$$

in which the added term is designed to account for degradation of the material along with Fickian diffusion, did not improve the fit (32). While there were not enough data points observed for these results to be considered a robust mathematical analysis, when considered along with the results of the characterization experiments it indicates there is little reaction between PEO and insulin. Instead almost all insulin contained in the mats is bound to CS and released through simple diffusion out of CS nanofibers.

Apart from the rate of insulin release, the bioactivity of the insulin delivered must be addressed. Dissolution in HFP, electrospinning, or dry storage could all potentially affect the bioactivity of insulin by degrading or denaturing the protein. While there are several signaling molecules the insulin signaling pathway that could have been measured, one of the major targets of the insulin signaling cascade is protein kinase B (Akt1) phosphorylation. Insulin causes Akt activation through insulin receptor substrate 1 (IRS1) phosphorylation, which activates phosphoinositide-3 kinase (PI3K). PI3K activates Akt1, which is responsible for many of the metabolic and mitogenic cellular responses to insulin stimulation. For this reason, cells exposed to bioactive insulin should contain a higher ratio of phosphorylated Akt (S473) to total Akt compared to cells exposed to standard culture medium. Adipocytes and preadipocytes in particular show a robust response to insulin, given their role as the body's major long term energy store. The response of the preadipocytes used in this study showed that insulin dissolved in HFP and electrospun into chitosan fibers undergoes no significant decrease in its bioactivity.

Transbuccal permeability was the only property of these fibers tested that did not show a dose-dependent relationship with polysaccharide content. In vitro experiments suggested that the CS:PEO20 fibers would have the highest short term insulin transport across the buccal mucosa simply by diffusion. While this was observed, the trend did not hold true for the other fiber blends. CS:PEO33 and CS:PEO50 fibers greatly underperformed the level of insulin delivery expected following the in vitro experiments. Hydrophilic compounds must cross the epithelium via the paracellular route through tight junctions between cells. Chitosan is able to enhance the permeability of epithelial membranes by transiently disrupting binding between tight junction proteins without causing cell death (33). Compared to synthetic options such as detergents it is considerably safer and more cost effective. Therefore, chitosan has been commonly incorporated into transmembrane drug delivery formulations as a permeation enhancer. Furthermore, mucoadhesive materials hold dissolved compounds in higher concentrations directly adjacent to the epithelium, encouraging diffusion across the membrane. While CS:PEO20 fibers were able to deliver promising levels of insulin across the buccal mucosa, the variation between samples was sub-optimal. It is possible this is a function of the tissues samples used and not the fibers themselves. Permeability of the buccal mucosa is known to vary widely throughout the



mouth and in ex-vivo studies it can be problematic to keep application sites constant (11). Future work will need to confirm this result in a more reproducible way by measuring the ability of CS:PEO fibers to lower blood sugar in a suitable animal model.

## Conclusions

In this work we have developed electrospun chitosan scaffolds designed for oral insulin delivery. Poly (ethylene oxide) was added in different ratios to control fiber morphology and physical properties. Degradation studies showed PEO dissolves rapidly under physiologic conditions leaving behind remodeled CS fibers. Higher chitosan:PEO ratio when spinning results in smaller fibers and more rapid insulin release. Insulin released from electrospun fiber mats shows no impaired bioactivity. CS:PEO20 fibers have 16 times higher buccal permeability compared to free insulin. Taken together, the results of this study suggest electrospun chitosan nanofibers can function as a viable vehicle for oral insulin delivery deserving of further study.

## Acknowledgments

This work was supported, in part, by NSF CAREER Award (CBET0954957) and NIH (R01EY024072). The authors acknowledge the technical advice of Dr. Leyuan Xu (Yale University) and Dr. W. Andrew Yeudall (Augusta University) on the project.

## References

1. Centers for Disease Control and Prevention. US Department of Health and Human Services; 2014. National diabetes statistics report: Estimates of diabetes and its burden in the United States.
2. Richardson T, Kerr D. Skin-related complications of insulin therapy. *American Journal of Clinical Dermatology*. 2003; 4(10):661–667. [PubMed: 14507228]
3. Hummel K, McFann KK, Realsen J, Messer LH, Klingensmith GJ, Chase HP. The increasing onset of type 1 diabetes in children. *The Journal of Pediatrics*. 2012; 161(4):652–657. [PubMed: 22578579]
4. Dabelea D, Mayer-Davis EJ, Saydah S, Imperatore G, Linder B, Divers J, Bell R, Badaru A, Talton JW, Crume T, Liese AD, Merchant AT, Lawrence JM, Reynolds K, Dolan L, Liu LL, Hamman RF. for the SEARCH for Diabetes in Youth Study. Prevalence of Type 1 and Type 2 Diabetes Among Children and Adolescents From 2001 to 2009. *JAMA*. 2014; 311(17):1778–1786. [PubMed: 24794371]
5. Soares S, Costa A, Sarmiento B. Novel non-invasive methods of insulin delivery. *Expert Opinion on Drug Delivery*. 2012; 9(12):1539–1558. [PubMed: 23098366]
6. Khafagy E, Morishita M, Onuki Y, Takayama K. Current challenges in non-invasive insulin delivery systems: A comparative review. *Advanced Drug Delivery Reviews*. 2007; 59(15):1521–1546. [PubMed: 17881081]
7. Cui F, Shi K, Zhang L, Tao A, Kawashima Y. Biodegradable nanoparticles loaded with insulin–phospholipid complex for oral delivery: Preparation, in vitro characterization and in vivo evaluation. *Journal of Controlled Release*. 2006; 114(2):242–250. [PubMed: 16859800]
8. Kumria R, Goomber G. Emerging trends in insulin delivery: Buccal route. *J Diabetol*. 2011; 2(1):1–9.
9. Salamat-Miller N, Chittchang M, Johnston TP. The use of mucoadhesive polymers in buccal drug delivery. *Advanced Drug Delivery Reviews*. 2005; 57(11):1666–1691. [PubMed: 16183164]
10. Sonia T, Sharma CP. An overview of natural polymers for oral insulin delivery. *Drug Discovery Today*. 2012; 17(13):784–792. [PubMed: 22521664]
11. Shojaei AH. Buccal mucosa as a route for systemic drug delivery: A review. *J Pharm Pharm Sci*. 1998; 1(1):15–30. [PubMed: 10942969]

12. Bobade NN, Atram SC, Wankhade VP, Pande DS, Tapar DK. A review on buccal drug delivery system. *Int J Pharm Sci Res.* 2013; 3:35–40.
13. Sill TJ, von Recum HA. Electrospinning: Applications in drug delivery and tissue engineering. *Biomaterials.* 2008; 29(13):1989–2006. [PubMed: 18281090]
14. Bowman K, Leong KW. Chitosan nanoparticles for oral drug and gene delivery. *International Journal of Nanomedicine.* 2006; 1(2):117–128. [PubMed: 17722528]
15. Jintapattanakit A, Junyaprasert VB, Kissel T. The role of mucoadhesion of trimethyl chitosan and PEGylated trimethyl chitosan nanocomplexes in insulin uptake. *Journal of Pharmaceutical Sciences.* 2009; 98(12):4818–4830. [PubMed: 19408295]
16. Krauland AH, Guggi D, Bernkop-Schnürch A. Oral insulin delivery: The potential of thiolated chitosan-insulin tablets on non-diabetic rats. *Journal of Controlled Release.* 2004; 95(3):547–555. [PubMed: 15023465]
17. Sarmento B, Ribeiro A, Veiga F, Sampaio P, Neufeld R, Ferreira D. Alginate/chitosan nanoparticles are effective for oral insulin delivery. *Pharmaceutical Research.* 2007; 24(12):2198–2206. [PubMed: 17577641]
18. Yin L, Ding J, He C, Cui L, Tang C, Yin C. Drug permeability and mucoadhesion properties of thiolated trimethyl chitosan nanoparticles in oral insulin delivery. *Biomaterials.* 2009; 30(29): 5691–5700. [PubMed: 19615735]
19. Yuan Q, Fu Y, Kao WJ, Janigro D, Yang H. Transbuccal delivery of CNS therapeutic nanoparticles: Synthesis, characterization, and in vitro permeation studies. *ACS Chemical Neuroscience.* 2011; 2(11):676–683. [PubMed: 22184511]
20. Zhang Y, Wei W, Lv P, Wang L, Ma G. Preparation and evaluation of alginate–chitosan microspheres for oral delivery of insulin. *European Journal of Pharmaceutics and Biopharmaceutics.* 2011; 77(1):11–19. [PubMed: 20933083]
21. Aduba DC, Hammer JA, Yuan Q, Yeudall WA, Bowlin GL, Yang H. Semi-interpenetrating network (sIPN) gelatin nanofiber scaffolds for oral mucosal drug delivery. *Acta Biomaterialia.* 2013; 9(5): 6576–6584. [PubMed: 23416578]
22. Xu L, Sheybani N, Ren S, Bowlin GL, Yeudall WA, Yang H. Semi-interpenetrating network (sIPN) co-electrospun gelatin/insulin fiber formulation for transbuccal insulin delivery. *Pharmaceutical Research.* 2015; 32(1):275–285. [PubMed: 25030186]
23. McClure MJ, Wolfe PS, Simpson DG, Sell SA, Bowlin GL. The use of air-flow impedance to control fiber deposition patterns during electrospinning. *Biomaterials.* 2012; 33(3):771–779. [PubMed: 22054536]
24. Marques MR, Loebenberg R, Almukainzi M. Simulated biological fluids with possible application in dissolution testing. *Dissolution Technol.* 2011; 18(3):15–28.
25. Pakravan M, Heuzey M, Ajji A. A fundamental study of chitosan/PEO electrospinning. *Polymer.* 2011; 52(21):4813–4824.
26. Snaveley WK, Subramaniam B, Rajewski RA, Defelippis MR. Micronization of insulin from halogenated alcohol solution using supercritical carbon dioxide as an antisolvent. *Journal of Pharmaceutical Sciences.* 2002; 91(9):2026–2039. [PubMed: 12210049]
27. Ohkawa K, Cha D, Kim H, Nishida A, Yamamoto H. Electrospinning of chitosan. *Macromolecular Rapid Communications.* 2004; 25(18):1600–1605.
28. Pillai C, Paul W, Sharma CP. Chitin and chitosan polymers: Chemistry, solubility and fiber formation. *Progress in Polymer Science.* 2009; 34(7):641–678.
29. Homayoni H, Ravandi SAH, Valizadeh M. Electrospinning of chitosan nanofibers: Processing optimization. *Carbohydrate Polymers.* 2009; 77(3):656–661.
30. Bhattarai N, Edmondson D, Veiseh O, Matsen FA, Zhang M. Electrospun chitosan-based nanofibers and their cellular compatibility. *Biomaterials.* 2005; 26(31):6176–6184. [PubMed: 15885770]
31. Yang H, Tyagi P, Kadam RS, Holden CA, Kompella UB. Hybrid dendrimer hydrogel/PLGA nanoparticle platform sustains drug delivery for one week and antiglaucoma effects for four days following one-time topical administration. *ACS Nano.* 2012; 6(9):7595–7606. [PubMed: 22876910]

32. Panyam J, Labhasetwar V. Biodegradable nanoparticles for drug and gene delivery to cells and tissue. *Advanced Drug Delivery Reviews*. 2003; 55(3):329–347. [PubMed: 12628320]
33. Rosenthal R, Günzel D, Finger C, Krug SM, Richter JF, Schulzke J, Amasheh S. The effect of chitosan on transcellular and paracellular mechanisms in the intestinal epithelial barrier. *Biomaterials*. 2012; 33(9):2791–2800. [PubMed: 22230222]

Author Manuscript

Author Manuscript

Author Manuscript

Author Manuscript

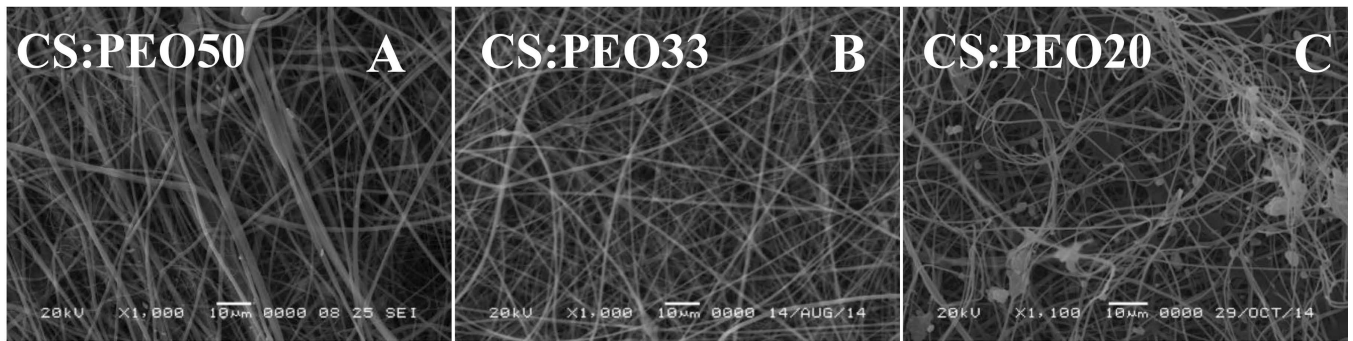


**Figure 1. At least 20% high molecular weight polymer is necessary for stable fiber formation** Poly (ethylene oxide) (Mw 900kDa) was added to dissolved chitosan electrospinning solution in decreasing ratios. At 20% PEO solution content intermittent beading can be observed. Scale bar 10µm.

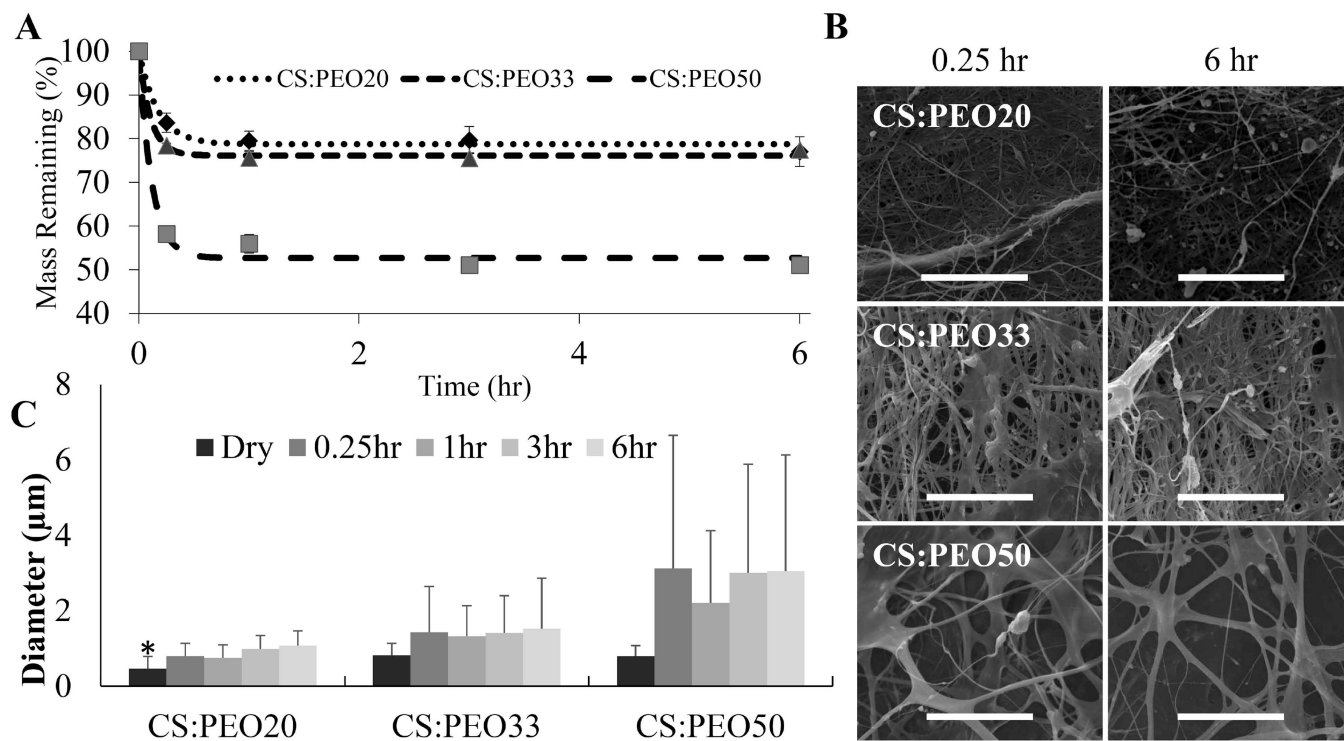


**Figure 2. CS:PEO fibers dissolve slowly under physiologic conditions**

10mg samples of CS:PEO fiber blends (n=3) were immersed in 5ml of PBS at 37°C. At predetermined time points PBS was removed. Samples were then washed once with diH<sub>2</sub>O and freeze dried overnight. Mass loss approximated PEO content (A). SEM micrographs showed no major morphological changes in fibers over the degradation period (B, scale bar represents 50 µm). The average fiber diameter measured in these micrographs also showed no significant changes within individual fiber blends after hydration (C). (\* denotes statistically significant difference between all groups  $p < 0.05$ )

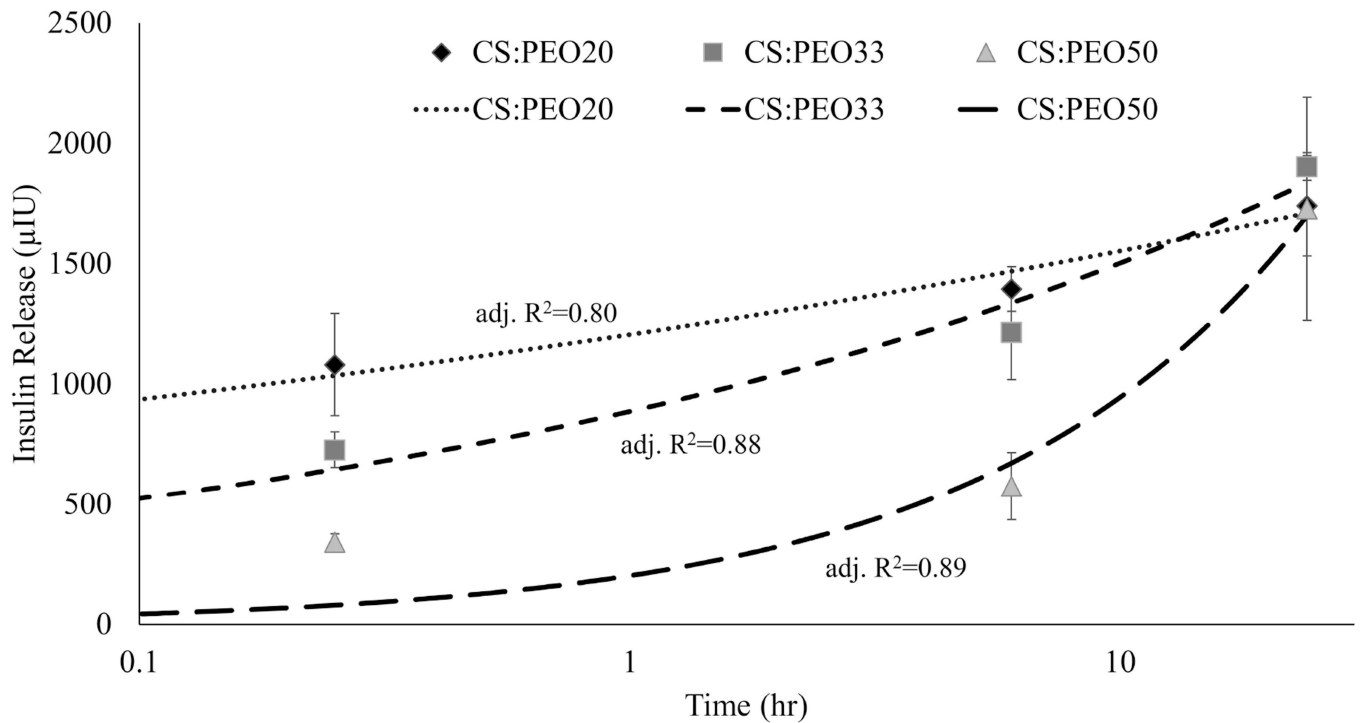


**Figure 3. Polysaccharide content controls insulin release kinetics**

Fiber blends of different chitosan:PEO ratios were immersed in PBS at 37°C. Insulin release was quantified at 15 minutes, 6 hours, and 1 day by ELISA assay. Various models were applied to fit the data. Curves corresponding to the Ritger-Peppas equation are shown. CS:PEO20 fibers show the fastest release profile, but there was no difference observed between blends at 24 hours.

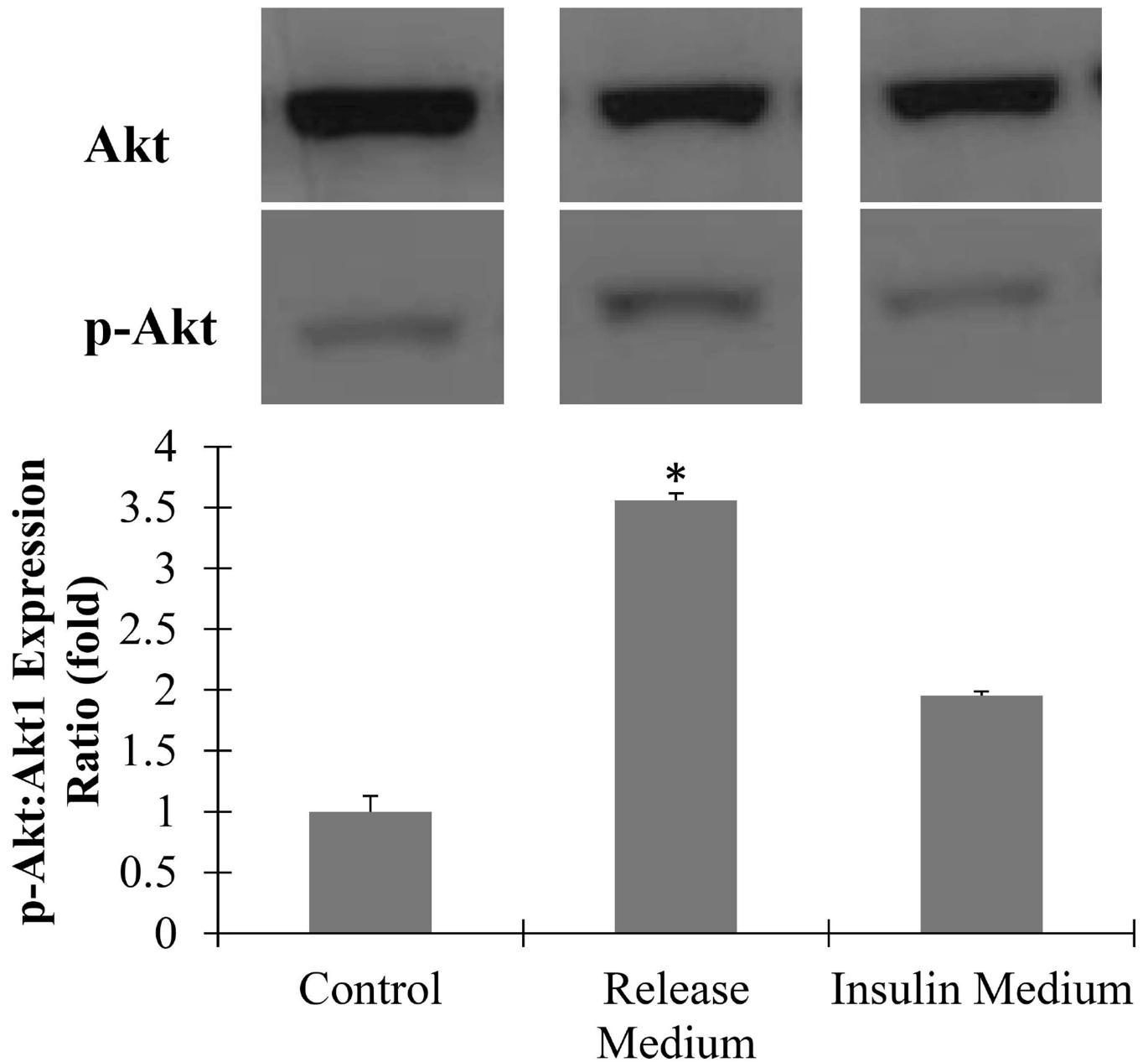


**Figure 4. Insulin remains bioactive after electrospun fiber fabrication**

3T3-L1 preadipocytes incubated for 10 minutes in either fresh growth medium (control), 6 hour CS:PEO20 fiber release medium, or insulin containing media (7.98  $\mu\text{g}/\text{mL}$ ). Western blots of cell lysates were run for p-Akt expression then stripped and re-probed for total Akt1 as loading controls. Cells exposed to fiber release medium showed 3.5 fold higher p-Akt/Akt expression ratio than control cells. (\* denotes statistically significant difference from all other groups  $p < 0.05$ )

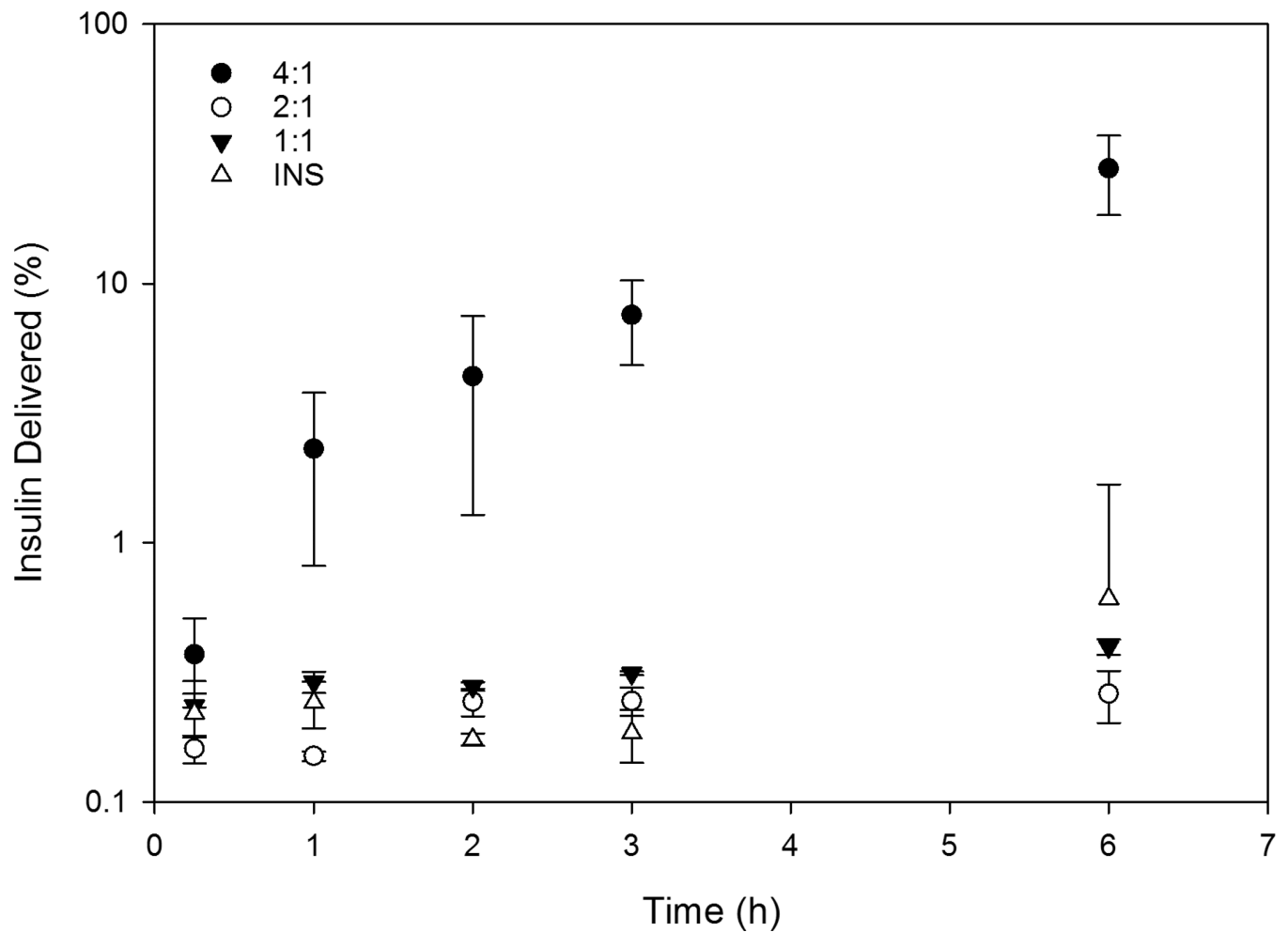


**Figure 5. Chitosan enhances insulin transbuccal permeability**

Insulin transport across the buccal membrane was determined using a Franz diffusion cell. Measurements of the insulin concentration of the acceptor chamber showed that membranes were largely impermeable to both dissolved insulin and the lower chitosan blend ratios, with those groups delivering less than 1% of their total protein over 6 hours. CS:PEO20 fibers however showed significantly higher insulin delivery over the other groups at all time points over 2 hours. The permeability coefficient of the buccal mucosa to each of these insulin compounds was calculated from the steady state flux region of the tests and CS:PEO20 fibers showed around a 500 fold increase in permeability over the other fiber blends and a 16 fold increase over naked insulin.



**Table 1**

Electrospinning solutions content and final INS content.

<b>Blend ratio</b>	<b>CS conc. (mg/mL)</b>	<b>PEO conc. (mg/mL)</b>	<b>INS conc. (mg/mL)</b>
CS:PEO20	8	2	0.4
CS:PEO33	8	4	0.4
CS:PEO50	8	8	0.4

Author Manuscript

Author Manuscript

Author Manuscript

Author Manuscript

**Table 2**

CS:PEO fiber mechanical properties.

<b>Blend Ratio</b>	<b>Peak Stress (Mpa)</b>	<b>Strain at Break (%)</b>
<b>CS:PEO20</b>	1.03±0.15	24.8±1.5
<b>CS:PEO33</b>	1.14±0.15	18.3±1.3
<b>CS:PEO50</b>	2.59±0.21	13.7±2.3

Author Manuscript

Author Manuscript

Author Manuscript

Author Manuscript

**Table 3**

Adjusted  $R^2$  and sum of squares due to error (SSE) for several simple models of drug release.

Blend Ratio	Higuchi (thin film diffusion) (Adj $R^2$ , SSE)	Ritger-Peppas (Fickian diffusion)	Peppas-Sahlin (Fickian diffusion + degradation)	Zero-Order
<b>CS:PEO20</b>	-2.66 1.004	0.80 0.047	0.83 0.048	-6.33 2.010
<b>CS:PEO33</b>	0.49 0.324	0.88 0.079	0.84 0.075	-0.40 0.885
<b>CS:PEO50</b>	0.88 0.134	0.89 0.114	0.89 0.098	0.86 0.157

**Table 4**

The insulin permeability coefficient and  $R^2$  of the cumulative flux curve for CS:PEO fiber blends and naked insulin.

<b>Blend Ratio</b>	<b>Permeability (<math>10^{-5}</math>cm/s)</b>	<b>Q-R<sup>2</sup></b>
<b>CS:PEO20</b>	0.255	0.74
<b>CS:PEO33</b>	0.127	0.61
<b>CS:PEO50</b>	21.5	0.97
<b>INS</b>	1.27	0.76

Author Manuscript

Author Manuscript

Author Manuscript

Author Manuscript